Carbon Dioxide Capture and Hydrogen Purification from Synthesis Gas by Pressure Swing Adsorption

Cheng-tung Chou [a]*, Fei-hong Chen [a], Yu-Jie Huang [a], Hong-sung Yang [b]

[a] Department of Chemical and Materials Engineering, National Central University, Jhong-Li, Taiwan
[b] Center for General Education, Hwa-Hsia Institute of Technology, Chung-Ho District, New Taipei City, Taiwan
t310030@ncu.edu.tw

Global warming has become more and more serious, which is caused by greenhouse gases. Cutting down the emission of CO_2 has already become one of the major research target in the world. This study utilized a pressure swing adsorption (PSA) process to separate high-purity hydrogen and to capture CO_2 from synthesis gas, which is the effluent stream of water-gas-shift reactor. The purified H_2 can be sent to gas turbine for generating electrical power or can be used for other energy source, whilst the CO_2 can be recovered and sequestrated to reduce greenhouse-gas effects. The PSA process studied is a two stage dual-bed eight-step process at room temperature using adsorbents: modified activated carbon AC5-KS and zeolite 13X-Ca. It is assumed that the gas mixture from which water has been removed enters the PSA process. The feed gas entering the PSA process consists of 1.3 % CO, 41.4 % CO_2 and 57.3 % H_2. It uses the method of lines combined with upwind differences, cubic spline approximation and LSODE of ODEPACK software to solve the equations. The optimal operating condition is obtained by varying the operating variables, such as feed pressure, bed length, step time, etc. Furthermore, the first stage H_2-PSA could achieve 99.98 % purity and 79 % recovery of H_2 as the top product and the second stage CO_2-PSA could obtain about 92 % purity and 98 % recovery of CO_2 as the bottom product. By PSA process, the goal of energy generation and environmental protection could be achieved at the same time.

1. Introduction

In recent years, increasing concentration of CO_2 in the atmosphere is requiring mankind to consider ways of controlling emissions of this greenhouse gas to the atmosphere. The United Nations Intergovernmental Panel on Climate Change (IPCC) has studied these problems and a general conclusion has been achieved between researchers, industry leaders, and politicians that dramatic reductions in greenhouse gas emissions must be achieved in order to stop climatic changes (IPCC, 2005; Abu-Zahra et al., 2009). So using coal more efficiently and turning it into a clean energy source is an important issue for the whole world. An integrated gasification combined cycle (IGCC) is a potential electric power technology that turns coal into synthesis gas, which can be burned to generate power. The CO composition in syngas reacts with steam to generate CO_2 and H_2 via the water-gas-shift reaction, $CO + H_2O \rightarrow CO_2 + H_2$. In this study pressure swing adsorption (PSA) is utilized to separate CO_2 and H_2 from the effluent of water-gas-shift reactor through H_2-PSA and CO_2-PSA at room temperature by two different adsorbents. PSA is a cyclic process that separates gas mixtures based on the difference of adsorption capacity of each component on an adsorbent. This technology consists of gas adsorption at high pressure and desorption at low pressure to produce high-purity products. As required by the U.S. Department of Energy, it is important to be able to concentrate the captured CO_2 into >90 % concentration that is suitable for underground storage.

 Yang et al.(1995) used a single-column PSA process with zeolite 5A to concentrate two binary systems, H_2/CO_2 and H_2/CO mixture (70/30 volume %), by experiment and simulation. The hydrogen could be concentrated from 70 % to 99.99 % (recovery 67.5 %) in the H_2/CO_2 system and to 97.09 % (recovery 67.5 %) in the H_2/CO system. Lopes et al. (2009) studied a new adsorbent for a PSA process; a commercial activated carbon (AC) was used for the preparation of a new material, AC5-KS, with enhanced capacity toward contaminants (CO_2, CH_4, CO, and N_2). Adsorption equilibrium and kinetics were studied on the modified AC and compared to the original AC results. An improvement of CO_2 adsorption capacity

of 17.5 % was observed at 303 K and 7 bar for sample AC5-KS. The adsorbent AC5-KS is also chosen as the adsorbent in this study. The purpose of this study is to concentrate the H_2 purity to higher than 99.9 % and to decrease the CO purity (<100ppm) for the use of fuel cell or other electrical power. Then CO_2 is expected to be recovered to reduce the green-house-gas effect. Figure 1 shows a conventional process scheme to produce hydrogen by coal gasification (Bell et al.,2011).
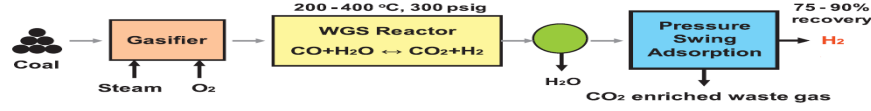

Figure1: Conventional process flow sheet for the production of hydrogen from coal gasification (Bell et al., 2011)

2. Methodology

2.1 Mathematical modelling
In the non-isothermal dynamic model, the following assumptions are made:
(1)   the linear driving force model is used because mass transfer resistance between the gas phase and solid phase exists.
(2)   the equilibrium adsorptive quantity is estimated by using the extended Langmuir isotherm equation.
(3)   the ideal gas law is applicable.
(4)   non-isothermal operation is considered.
(5)   only axial concentration and temperature gradient are considered.
(6)   the pressure drop along the bed can be neglected due to large particle size.

These assumptions are used in the following equations:
Overall mass balance:
$$-\frac{\partial q}{\partial z} = \frac{\varepsilon A}{R}\frac{\partial (P/T)}{\partial t} + (1-\varepsilon)A\sum_{i=1}^{n}\frac{\partial n_i}{\partial t}$$
(1)

Mass balance for component i:
$$\frac{\partial}{\partial z}\left(\frac{\varepsilon A D_{ax,i}P}{RT}\frac{\partial y_i}{\partial z}\right) - \frac{\partial (y_i q)}{\partial z} = \frac{\varepsilon A}{R}\frac{\partial}{\partial t}\left(\frac{y_i P}{T}\right) + (1-\varepsilon)A\frac{\partial n_i}{\partial t}$$
(2)

Energy balance:
$$\left(A\bar{k}\right)\frac{\partial^2 T}{\partial z^2} - \frac{\partial}{\partial z}\left(\bar{C}_p qT\right) - \pi Dh(T-T_\infty)$$
$$= \frac{\varepsilon A}{R}\frac{\partial}{\partial t}\left(\bar{C}_p P\right) + (1-\varepsilon)A\sum_{i=1}^{n}\frac{\partial}{\partial t}\left[n_i\left(\tilde{C}_{pi}T - H_i\right)\right] + (1-\varepsilon)\rho_s\hat{C}_{ps}A\frac{\partial T}{\partial t}$$
(3)

Extended Langmuir-Freundlich isotherm equation:
$$n_i^* = \frac{\rho_s q_{m,i} b_i y_i^{n_i} P^{n_i}}{1+\sum_{j=1}^{n} b_j y_j^{n_j} P^{n_j}}$$
(4)

where
$$q_{m,i}=a_{i,1}+\left(a_{i,2}\times T\right)\quad n_i = n_{i,1}+\left(n_{i,2}/T\right)\quad b_i = b_{i,0}\exp\left(b_{i,1}/T\right)$$

Linear driving force model:
$$\frac{\partial N_i}{\partial t} = K_{LDF}\left(N_i^* - N_i\right)$$
(5)

Linear driving force coefficient (Malek et al.,1997):
$$\frac{1}{K_{LDF}} = \frac{R_p}{3k_f}\frac{n_i^*\rho_s}{C_i} + \frac{R_p^2}{15\varepsilon_p D_{eff}}\frac{n_i^*\rho_s}{C_i} + \frac{r_c^2}{15D_c}$$
(6)

Micropore diffusivity:
$$\frac{D_c}{r_c^2} = \frac{D_c^0}{r_c^2}\exp\left(-\frac{E_a}{RT}\right)$$
(7)

Twenty-one basic grid points are marked in the bed to set up the initial concentration, initial temperature, and initial pressure. The partial differential equations are converted to ordinary differential equations by the method of lines. The spatial derivatives of the concentration and the gas temperature are evaluated by upwind differences at every grid point. The cubic spline approximation is used to estimate the flow rates in the adsorptive bed. The concentration, temperature, and adsorption quantity in the bed are integrated with respect to time by LSODE of ODEPACK software with a time step of 0.1s. The simulation is stopped by using Eq. 8 when the system reaches a cyclic steady state.

$$\sum (1 - \frac{Y(last\ cycle)}{Y(this\ cycle)})^2 < 1 \times 10^{-4}$$

(8)

2.2 PSA process

The PSA process studied is a two stage dual-bed eight-step process at room temperature using adsorbents: modified activated carbon AC5-KS and zeolite 13X-Ca. The feed gas is from the effluent stream in the water-gas-shift reactor which is cited in the report of National Energy Technology Laboratory (NETL Report, 2009). It is assumed that the gas mixture from which water has been removed enters the PSA process. Furthermore, the feed gas entering the PSA process consists of 1.3 % CO, 41.4 % CO_2 and 57.3 % H_2. The process is described as follows: feed pressurization (I), high pressure adsorption (II), continuous adsorption (III), continuous adsorption (IV), countercurrent depressurization (V), continuous depressurization (VI), countercurrent purge (VII), and product pressurization (VIII). During step I to step IV, the bed pressure increases from atmospheric pressure to high pressure, and less adsorptive hydrogen is produced. Strongly adsorptive carbon monoxide and carbon dioxide are produced during step V to step VII when the bed pressure decreases from high pressure to low pressure (0.1 atm). In step VII and step VIII, we use the less adsorptive product to purge and pressurize the bed from low pressure to atmospheric pressure. The procedure of the dual-bed eight-step process is shown in Figure 2. The physical parameters of adsorption bed and the step time for two stages are shown in Tables 1 and 2.
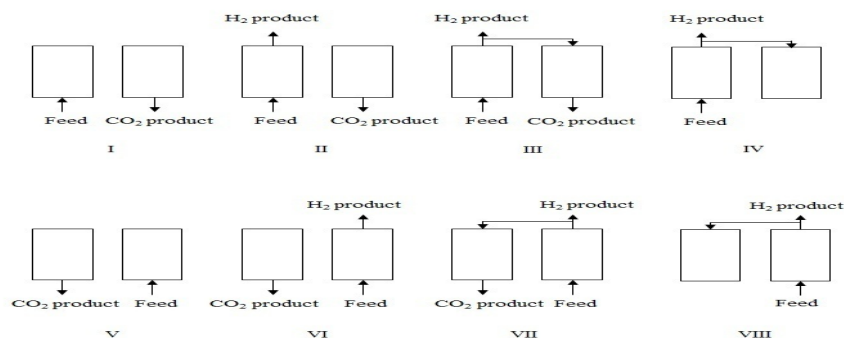
Figure 2: Procedure of the dual-bed eight-step PSA process.

Table 1: Step time for two stages

Step time(s)	I	II	III	IV	V	VI	VII	VIII
H_2-PSA	20	25	10	10	20	25	10	10
CO_2-PSA	150	50	10	10	150	50	10	10

Table 2: Physical parameters of bed

Bed length(cm)	730
Bed diameter(cm)	240
Operating temperature	303K
Feed pressure	7atm
Vacuum pressure	0.1atm

3. Results and discussion

3.1 Adsorption isotherms of 13X-Ca and AC5-KS

The adsorption isotherms of CO, CO_2 and H_2 on 13X-Ca and AC5-KS were measured by Lopes et al. (2009, 2010). The adsorption data were fitted by employing the extended Langmuir-Freundlich isotherm equation in this study. The fitting parameters are detailed in Table 3.

Table 3: Langmuir-Freundlich isotherm fitting parameters of CO, CO_2 and H_2 on 13X-Ca and AC5-KS

	AC5-KS	13X-Ca
CO		
$a_{i,1}$(mole/Kg)	16.4	-1.36
$a_{i,2}$(mole/K $\cdot$ Kg)	4.47×10^{-5}	2.32×10^{-2}
$b_{i,0}$(1/bar)	9.397×10^{-5}	9.36×10^{-4}
$b_{i,1}$(K)	2.292×10^{3}	1.583×10^{3}
$n_{i,1}$(-)	1.599	2.63×10^{-1}
$n_{i,2}$(K)	-277.975	79.505
CO_2		
$a_{i,1}$(mole/Kg)	25.1	1.64
$a_{i,2}$(mole/K $\cdot$ Kg)	-4.18×10^{-2}	1.33×10^{-2}
$b_{i,0}$(1/bar)	9.719×10^{-5}	6.566×10^{-5}
$b_{i,1}$(K)	1.856×10^{3}	3.204×10^{3}
$n_{i,1}$(-)	1.675	-1.218
$n_{i,2}$(K)	-275.04	576.276
H_2		
$a_{i,1}$(mole/Kg)	6.57	-0.649
$a_{i,2}$(mole/K $\cdot$ Kg)	3.70×10^{-2}	1.96×10^{-2}
$b_{i,0}$(1/bar)	4.338×10^{-6}	6.797×10^{-6}
$b_{i,1}$(K)	1.913×10^{3}	2.042×10^{3}
$n_{i,1}$(-)	2.652	1.43
$n_{i,2}$(K)	-527.941	-158.364

## 3.2 Dual-bed 8-step PSA process simulation

In this study, the optimal operating conditions are discussed by varying the operating variables, such as feed pressure and bed length.

Bed length at H_2-PSA: All the operating variables are fixed except bed length. The amount of adsorbent increases when bed length increases. Figure 3 shows that as bed length increases, the H_2 recovery decreases since the hydrogen flow to the top product decreases. At the same time, the CO_2 flow to the top product decreases, so that H_2 purity increases. When the amount of adsorbed gas increases, the gas flow to the bottom product increases during desorption. The CO_2 purity in the bottom product decreases since the recovery of H_2 increases in the bottom product.
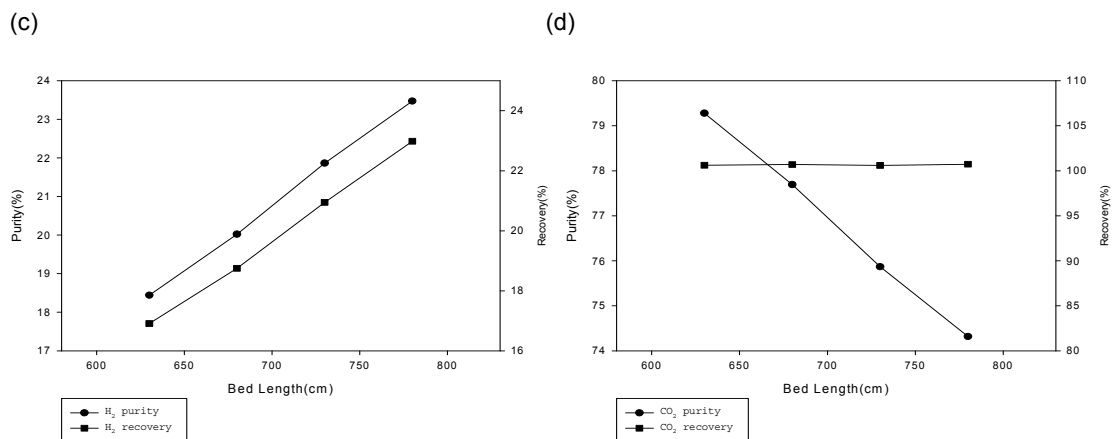
(a)   (b)

(c)

(d)
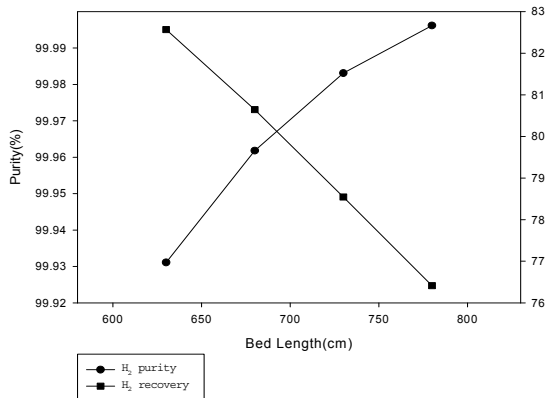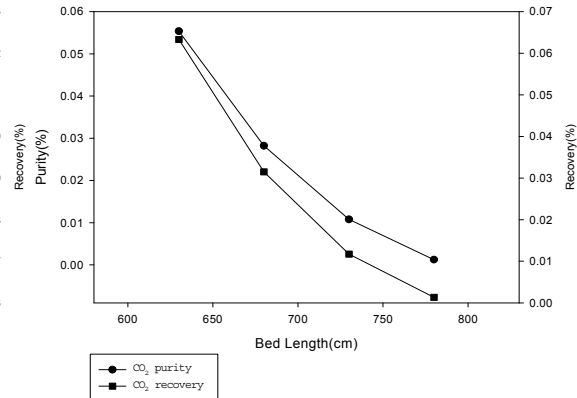
Figure 3: Effect of bed length at H$_2$-PSA *on (a) H$_2$ in top product (b) CO$_2$ in top product (c) H$_2$ in bottom product (d) CO$_2$ in bottom product*

Feed pressure at CO$_2$-PSA: All the operating variables such as vacuum pressure, bed length, feed rate and step time are fixed, except for feed pressure. Because the amount of gas adsorbed on 13X-Ca increases as feed pressure increases, the flow of the strong adsorptive component to the bottom of the bed during desorption increases. Figure 4 shows that as feed pressure increases, the CO$_2$ purity and recovery in top product decreases because CO$_2$ adsorption quantity becomes larger. Furthermore, the H$_2$ recovery in top product decreases since the amount of H$_2$ adsorbed increases and the H$_2$ purity in top product increases because the amount of CO and CO$_2$ decreases in top product. As feed pressure increases, the CO$_2$ purity in bottom product decreases as the amount of H$_2$ flows to bottom increases.
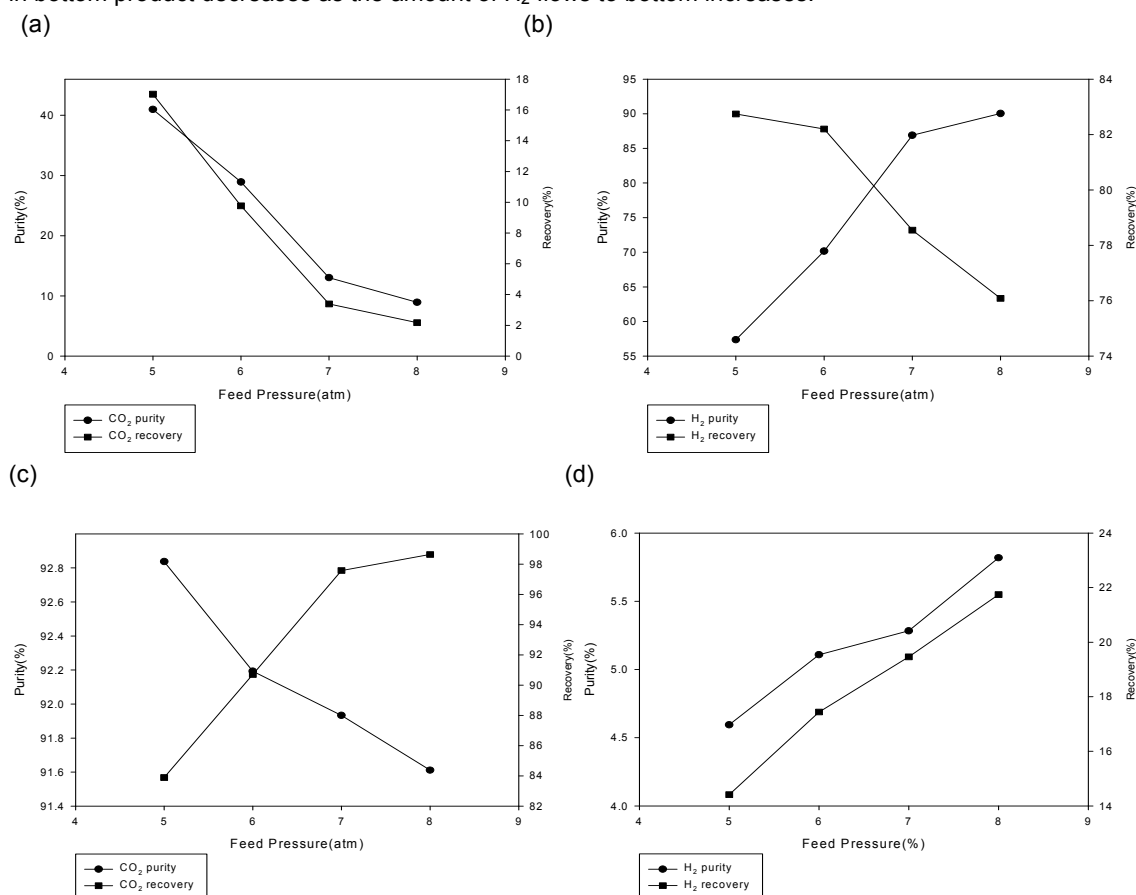
(a)

(b)

(c)

(d)

Figure 4: Effect of feed pressure at CO$_2$-PSA *on (a) CO$_2$ in top product (b) H$_2$ in top product (c) CO$_2$ in bottom product (d) H$_2$ in bottom product*

Pressure swing adsorption (PSA) is utilized to capture CO_2 from the exit stream of water-gas-shift reactor at room temperature. The best operating conditions for the 2-bed 8-step PSA process at room temperature is shown in Figure 5. The results of best operating condition for the dual-bed 8-step process at room temperature are 99.98 % purity and 78.55 % recovery of H_2 as top product, and 91.97 % purity and 97.8 % recovery of CO_2 as bottom product as shown in Figure 5.
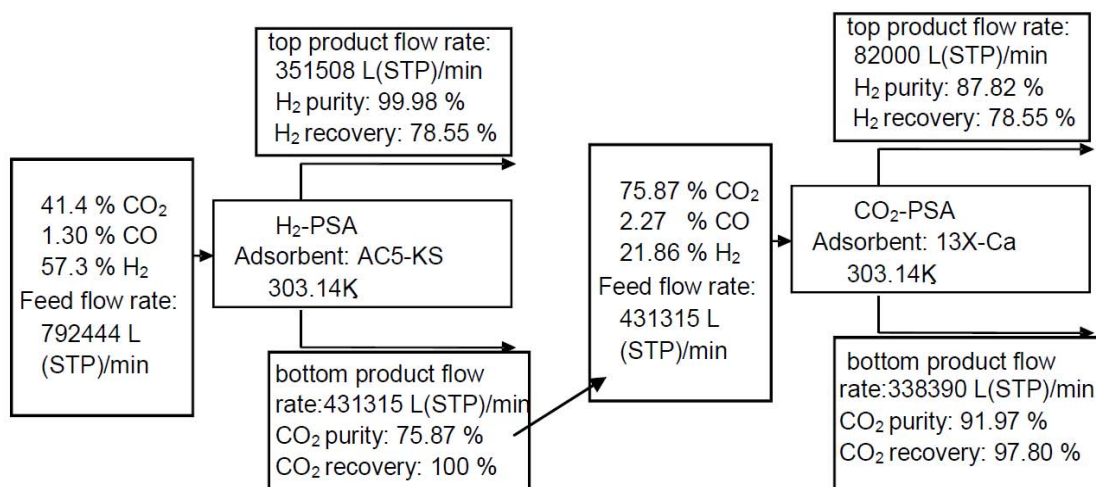

Figure 5: Results of the two stages of the 2-bed 8-step PSA process at room temperature

4. Conclusion

This study can obtain high purity of CO_2 through second stage by 13X-Ca. The purified H_2 through first stage by AC5-KS can be sent to gas turbine for generating electrical power or can be used for other energy source. It is assumed that the gas mixture from which water has been removed enters the PSA process. The optimal operating condition is obtained by varying the operating variables, such as feed pressure, bed length, etc. Furthermore, the first stage H_2-PSA could achieve 99.98 % purity and 79 % recovery of H_2 as the top product and the second stage CO_2-PSA could obtain about 92 % purity and 98 % recovery of CO_2 as the bottom product. By PSA process, the goal of energy generation and environmental protection could be achieved at the same time.

Acknowledgement

Reference

Abu-Zahra M.R.M., Feron P.H.M., Jansens P.J., Goetheer E.L.V., 2009, New process concepts for CO_2 post-combustion capture process integrated with co-production of hydrogen, International J. of Hydrogen Energy, 34, 3992-4004.

Bell D.A., Towler B.F, Fan M., 2011, Coal gasification and its applications, Elsevier, London, UK.

IPCC (Intergovernmental Panel on Climate Change), 2005, Carbon dioxide capture and storage, Cambridge University Press.

Lopes F. V. S., Grande C. A., Ribeiro A. M., Oliveira E. L. G., Loureiro J. M., Rodrigues A. E., 2009, Enhancing capacity of activated carbons for hydrogen purification, Ind. Eng. Chem. Res., 48(8), 3978–3990.

Lopes F. V. S., Grande C. A., Ribeiro A. M., Vilar V. J. P., Loureiro J. M., Rodrigues A. E., 2010, Effect of Ion exchange on the adsorption of steam methane reforming off-gases on zeolite 13X, J. Chem. Eng. Data, 55(1), 184–195.

Malek A., Farooq S., 1997, Kinetics of hydrocarbon adsorption on activated carbon and silica gel, AIChE J., 43(3),761–776.

NETL (The United States Department of Energy, National Energy Technology Laboratory), 2009, Evaluation of Alternate Water Gas Shift Configurations for IGCC Systems, DOE/NETL-401/080509.

Yang J., Han S., Cho C., Lee C.H., Lee H., 1995, Bulk separation of hydrogen mixtures by a one-column PSA process, Separations Technology, 5(4), 239-249.